EVALUATION OF SOLAR CELL COVERS AND ENCAPSULANT MATERIALS FOR SPACE APPLICATION*

Dennis A. Russell
Boeing Aerospace Company
Seattle, Washington

SUMMARY

Testing of covered or encapsulated solar cells employing new materials and methods is described. Cover materials evaluated include glass resins, 2-mil glass applied with adhesives or electrostatically bonded and thin plastic films of FEP or PFA applied with adhesive. Solar cells were exposed to environmental conditions simulating those encountered in outer space. These test conditions include 1 MeV electrons, 0.5 MeV protons and thermal cycling in vacuum. During testing the solar cells were monitored for variations in electrical characteristics and structural changes.

INTRODUCTION

The ever increasing emphasis on high power/weight ratio of solar cell arrays and improved economy of manufacture of these structures requires new efforts to investigate methods in the application of light materials suitable for use as solar cell covers. The general objective of this program is to evaluate the effects of space radiation (electrons, protons, and ultraviolet), vacuum and thermal cycling on a variety of solar cell covers applied to solar cells. The approach is to expose groups of individual cells and cell modules encapsulated or covered with various materials to environmental conditions simulating those encountered during 10 years in geosynchronous orbit.

In this paper the test systems and methods used to simulate the space environments are presented. Test results from the electron irradiations interspersed with thermal cycling and proton irradiations interspersed with thermal cycling are presented including photographs of test cells.

SYSTEMS AND METHODS

Electron and Proton Irradiation

The Boeing Radiation Effects Laboratory's Dynamitron particle accelerator was the source of both the 1.0 MeV electrons and the 0.5 MeV protons used in

*This work was supported by NASA-Lewis under contract NAS3-22222.

this study. Basically the particle beam after being analyzed by a 90 degree bending magnet, is directed into an evacuated chamber where it impinges on a high-purity aluminum foil. The thickness of the scattering foil is selected to give the desired profile for the scattered particle field at the sample plane. The incident particle beam is adjusted in energy so that, after losing energy in traversing the scattering foil, the particles emerge with the desired energy on the sample plane. The scattered particle field is mapped using a remotely controlled rotating Faraday cup. The incident flux profile on the sample plane is then determined from this relative beam profile and absolute intensities measured by a Faraday cup located in the sample plane. Fluences are then obtained by integrating the current collected at the sample plane or by timing the exposure.

UV Exposure

At the time of the writing of this paper the UV vacuum test chamber is being setup. The UV exposure will be done at a four equivalent UV sun rate. The UV source will be a Spectrolab X25L Solar Simulator. The vacuum chamber and simulator will be setup to operate continuously except when I-V measurements or thermal cycling is required.

Thermal Cycling

The test cells were mounted on a 1/8-inch thick copper plate with small beryllium-copper clips. Figure 1 is a view of the test cells mounted on the copper plate in the test chamber. A thin layer of thermal heatsink compound was placed between each cell and the copper plate to ensure good thermal conductivity. The sample plate was attached to a copper thermal control plate equipped with integral resistance heaters and cooling tubes. The back of this plate is shown in figure 2.

During thermal cycling the sample plate assembly was rotated 90° and the thermal cycling cover plate also containing integral resistance heaters and cooling tubes was moved into close proximity of the sample plate assembly (fig. 3). This method insures that the test cells were thermal cycled regardless of the thermal conductivity of the encapsulated cells. The cells were cycled from -175°C to +55°C. Liquid nitrogen was run through both plates to obtain the lower limit of 175°C. To warm the cells to 55°C a combination of the resistance heaters and hot gas was used. The cycling was conducted with a five-minute soak at both -175°C and +55°C. The heating rate was controlled within 10°C/min to 13°C/min and the cooling rate controlled within 10°C/min to 20°C/min.

I-V Measurements

I-V measurements were made both ex situ and in situ. The ex situ measurements were made before the start of irradiation and after the completion of all irradiation and thermal cycling. The in situ measurements differ from the ex situ measurements only in that the solar simulator is beamed through a GE124 optical-grade fused silica window and the intensity is monitored by two monitor cells located in the vacuum test chamber but protected from the irradiation. The same Spectrolab X25L solar simulator with an AM0 close-match filter was used for both the ex situ and in situ measurements. The I-V measurements were made at a nominal 25°C.

The data acquisition and reduction system consisted of a Tektronix 4051 minicomputer and graphics system. The 4051 was used to drive a load bank, store the raw data and analyze the data. A Tektronix 4662 plotter was used to plot computer fitted I-V and power curves and list I_{sc}, V_{oc}, P_{Max} and the fill factor for each level. Figures 4 and 5 are examples of a computer-plotted family of I-V and power curves.

Temperature Monitoring and Control

Test cell temperature was monitored by attaching a copper-constantan, Type T, thermocouple with epoxy to the surface of representative cells in each run. The temperature of the sample plate was also monitored.

During the I-V measurements the sample plate temperature and cell surface temperatures differed by 2°C to 8°C with the majority of cells differing by 3°C to 5°C. In order to bring the majority of cells to 25°C $\pm$1°. The sample plate temperature was reduced to 22°C. A temperature controlled water bath was used to control the sample plate temperature during both the I-V measurements and the irradiations. All particle irradiations were done at 55°C $\pm$ 5°.

TEST CONDITIONS

Table 1 lists both the electron and proton test conditions by stress level. Each level is either an irradiation or a set of 15 thermal cycles. I-V measurements were taken at each stress level. Visual inspection of the physical integrity of the cell was also made at each stress level. In situ photographs were taken of one representative cell of each type before testing and of each cell after testing.

TEST RESULTS

There were eight types of covers or encapsulants on cells in the testing. The cover materials included Glass Resins, 2-mil glass applied with adhesives or electrostatically bonded and thin plastic films such as FEP or PFA applied with adhesive. Table 2 lists the cell type designation and the components of the cell system including the cover, back, cell and adhesive used.

A-Series

(8-10 mils thick cell, 4-mil 0211 Ceria-doped cover, no backing, 0.5-mil 93-500 adhesive)

Electron Irradiation. The cells showed only normal behavior during irradiation or thermal cycling. Figure 6 is a plot of the average normalized maximum power versus fluence. (Where there are two data points at the same fluence value there has been a set of 15 thermal cycles run on the cells. Table 1 indicates at which fluences the thermal cycles have been performed.)

Proton Irradiation. There was no visible damage to the cells throughout the test. Figure 7 shows that the thermal cycling at 3×10^{14} P/cm^2 and 3.3×10^{15} P/cm^2 did not change the maximum power and that the 4-mil 0211 Ceria-doped cover protected the cell from proton damage.

C-Series

(2-mil cell, 2-mil FEP-A cover, 1-mil Kapton back, 2-mil 93-500 adhesive front and back)

Electron Irradiation. The first visible damage was observed after a fluence of 5×10^{15} e/cm^2 and 30 thermal cycles. At this point the FEP-A covers started cracking loose from the cell. Before this point there was no visual damage observed; therefore, the second set of 15 thermal cycles induced the cracking of the FEP-A. The cracking became worse after the third set of thermal cycles were completed. Figure 8 is a photograph of a cell after the complete irradiation schedule. The FEP-A has many small cracks and is raised up from the cell in many places. Figure 9 shows that after the second and third sets of thermal cycles there was a 2% reduction in maximum power due to light scattering from the cracks.

Proton Irradiation. The only visible and electrical damage observed was after a total fluence of 3.3×10^{15} p/cm^2. This caused the cell to have a hazy or foggy appearance and a loss of 3% in maximum power as shown in figure 10. This loss was due to a 3% decrease in I_{sc}. There was no observable damage directly caused by thermal cycling.

D-Series

(8-mil cell, ∿1.5-mil 93-500 cover, no backing no adhesive)

Electron Irradiation. There was only normal behavior observed electrically or visually. Figure 11 shows that thermal cycling did not affect the maximum power even after a fluence of 1×10^{16} e/cm^2.

Proton Irradiation. Cracks started to show in the 93-500 after 3×10^{14} p/cm^2 without any thermal cycling. The rest of the proton fluence and thermal cycling caused further cracking until the 93-500 looked like "alligator skin." It appears that the 93-500 hardened in the proton beam. Figure 12 is a photograph after the completed proton irradiation. Figure 12 indicates that the cracks allowed large electrical damage to occur.

E-Series

(10-mil cell, 2-mil GE 615/UV-24 cover, no backing, no adhesive)

Electron Irradiation. There was no unusual behavior observed electrically or visually. Figure 14 indicates that the first set of thermal cycles caused some improvement in the maximum power and further cycling did not affect the power.

Proton Irradiation. Cracks started to show in the GE cover material after the first set of thermal cycles. The rest of the proton fluence and thermal cycling caused further cracking until the GE 615/UV-24 looked like "alligator skin" similar to the D-Series cells. Figure 15 is a photograph after the completed proton irradiation. Figure 16 shows that thermal cycling improved cell performance slightly and that the cracks in the covering caused protons to reach the cell and degrade it.

P-Series (Pantek Cell)

(2-mil cell, 0.5-mil GR650 cover, no backing, no adhesive)

Electron Irradiation. The cells showed no visible damage until they received 5×10^{15} e/cm^2 and 30 thermal cycles. At this point four cells were cracked with parts of the cell broken out on two of them. At the completion of the electron irradiation there were two cells with additional parts broken out (fig. 17), one cell with no more damage than a crack and two cells with no visible damage at all. Figure 18 shows that initially thermal cycling improved the cells output. However, by a fluence of 1×10^{16} e/cm^2 the thermal cycles had no effect.

Proton Irradiation. Three of the five cells exhibited cracks after the first set of thermal cycles and by the completion of the test schedule a fourth cell cracked. The power output of the cell degraded tremendously during the first irradiation (fig. 19) There was no visible damage to explain the loss of output at that point. It is clear that the GR 650 cover is not thick enough to stop the protons. Figure 20 is a photograph showing the cracks in the cells at the completion of testing.

GE Cells

(2-mil cell, 2-mil PFA "hard-coated" cover, 1-mil Kapton backing, 93-500 front and back adhesive)

Electron Irradiation. The GE cells all had bubbles trapped in the encapsulant before mounting in the test chamber. The edges of the cells would not lay flat on the sample plate. The cells exhibited no visible damage until they had received a total fluence of 1×10^{15} e/cm^2 and 15 thermal cycles. At this point three cells had cracks in the PFA cover material. After a total fluence of 5×10^{15} e/cm^2 and 30 thermal cycles, the PFA covers on four cells had many cracks and three of the four cells were cracked by curling during thermal cycling. After a total fluence of 1×10^{16} e/cm^2 and 45 thermal cycles all the cells and PFA covers were badly cracked (fig. 21). The PFA and Kapton had become very brittle.

There is no electrical data after the 5×10^{15} e/cm^2 fluence because the cells were broken and shorted-out (fig. 22).

Proton Irradiation. The GE cells showed visible damage after the first proton fluence of 3×10^{14} p/cm^2 and no thermal cycling. Four of the five cells had started to curl up from the contact bar end. One cell's cover had started to blister. After the first 15 thermal cycles the only additional damage was more curling. After a total fluence of 3.3×10^{15} p/cm^2 and 15 thermal cycles the PFA covers were blistered and peeling off on all five cells. The last 15 thermal cycles only made the blistering and peeling worse. Figure 23 is a photograph showing the blistering and peeling after the completed proton test.

The maximum power plot (fig. 24) shows that after the first set of thermal cycles the PFA cover had peeled enough to allow protons to damage the cell. The data point for the last set of thermal cycles is an average of one point because only one cell had an output, therefore it is of little significance.

Double-Number Cells

(2-mil cell; 2-mil 0211 cover; 2-mil FEP-20C, 1 1/2-mil fiberglass, 2-mil FEP-20C and 1-mil Kapton backing; 2-mil FEP-A adhesive)

Electron Irradiation. There was a slight haze when viewed at an angle between the covers and the cells and one cover was cracked after the first set of thermal cycles. The next visible damage occurred after a total fluence of 1×10^{16} e/cm^2 in which two more cells had cracked covers. After the final set of thermal cycles the cell-cover interface looked hazy when viewed at an angle and it appeared the covers were coming loose. When the cells were removed from the chamber it was found that the ends of the cells had curled up from the sample plate. The maximum power plot (fig. 25) shows that the last set of thermal cycles caused a 15% decrease due to the reduced light through the hazy adhesive and poor thermal contact to sample plate.

Proton Irradiation. The cells exhibited no visible damage during the entire proton test. There was essentially no electrical damage either (fig. 26).

Electrostatically Bonded Cells

(2-mil cell, 2-mil 7070 cover electrostatically bonded) (Reference 1)

Electron Irradiation. The ESB cells showed no visible damage until they had received a total fluence of 1×10^{15} e/cm^2 and 15 thermal cycles. At this point four of the five cells had cracks in the cover or portions of the cover were missing or coming loose. After a total fluence of 1×10^{16} e/cm^2 and 45 thermal cycles the damage became worse with the cover coming loose on two cells. One cell displayed no visible damage throughout the test. Figure 27 is the maximum power versus fluence plot showing the effects of the thermal cycling. It should be mentioned that the cells used in this test were some of the first cells made during the parameter optimization phase of the electrostatic bonding program (ref. 1) did not have the quality bond that was later achieved.

Proton Irradiation. No visible damage was observed until after the first set of thermal cycles. At this point two of the five cells had cracked and had a reduced output or no output at all. There were no further changes in the cell appearance until the testing was completed. At this point, two cells showed no change from the beginning of the test except some curling on the ends, two cells were cracked and curled and had no output and one cell was curled and had several lengthwise cracks in the glass. Figure 28 indicates no electrical damage caused by the protons.

2-mil 7070 Glass

Samples of 2-mil 7070 glass 2 cm x 2 cm in size were also included in the electron and proton irradiations. The glass will be returned to NASA-Lewis for transmission measures.

Electron Irradiations. There was no visible damage to the glass throughout the electron irradiation.

Proton Irradiation. The glass started to curl on the ends which were not held down after the first set of thermal cycles and 3×10^{14} p/cm^2 fluence. The curling continued throughout the test. The glass curled up as much as 5-mm off the surface of the plate at the ends. It is thought that the protons may be compacting the glass at the surface, changing its density and causing the curling.

CONCLUSIONS

There are a few general conclusions that can be reached now without more extensive reduction of the electrical data and the completion of the UV testing.

1. The A-Series cell which is the more standard type of cell withstood the electron and proton environments very well, as would be expected.

2. The cells coated with only 93-500 (D-Series) or GE 615/UV-24 (E-Series) have no chance of surviving the proton environment.

3. The Pantek cell (P-Series) with a thin coating of GR 650 will not survive the proton environment because of either pin holes in the coating or just not enough of it. The cell also tended to break apart during thermal cycling.

4. The C-Series cell's 2-mil FEP-A cover came loose in the electron environment.

5. The PFA "hard-coated" GE cells did not withstand the combination of proton irradiation and thermal cycling.

6. The ESB cells showed promise in the electron environment due to the fact that one of the better quality bonded cells showed no physical damage and normal electrical degradation. The ESB cells withstood the proton environment well.

7. For the Double-Number cells, it appears that the FEP-A adhesive became hazy and would not hold the cover in the electron environment.

REFERENCE

1. Egelkrout, D. W.; Horne, W. E.: Electrostatic Bonding of the Thin (~3 mil) 7070 Cover Glass to Ta_2O_5 AR-Coated Thin (~2 mil) Silicon Wafers and Solar Cells. 4th HERD Solar Cell proceedings, 1980.

TABLE 1. ELECTRON AND PROTON TEST CONDITIONS

STRESS LEVEL	ELECTRON TEST: TOTAL ELECTRON FLUENCE (e/cm^2)	ELECTRON TEST: TOTAL NUMBER THERMAL CYCLES	PROTON TEST: TOTAL PROTON FLUENCE P/cm^2	PROTON TEST: TOTAL NUMBER THERMAL CYCLES
0	0	0	0	0
1	5×10^{14}	0	3×10^{14}	0
2	1×10^{15}	0	3×10^{14}	15
3	1×10^{15}	15	3.3×10^{15}	15
4	5×10^{15}	15	3.3×10^{15}	30
5	5×10^{15}	30		
6	1×10^{16}	30		
7	1×10^{16}	45		

TABLE 2. CELL TYPE DESIGNATION

DESIGNATION	CELL THICKNESS (mils)	COVER	BACK	ADHESIVE
A-Series	8-10	4 mil 0211 ceria doped	None	93-500 ∿0.5 mil
C-Series	∿2	2 mil FEP-A	1 mil Kapton	93-500 ∿2 mil ea. front and back
D-Series	∿8	∿1.5 mil 93-500	None	None
P-Series	∿2	∿0.5 mils GR650	None	None
GE Cells	∿2	2 mil PFA "Hard-coated"	1 mil Kapton	93-500 front and back
Double Number Cells	2	2 mil 0211	2 mil FEP-20C 1 1/2 mil Fiberglass 2 mil FEP-20C 1 mil Kapton	2 mil FEP-A
E-Series	∿10	2 mil GE 615/UV-24	None	None
ESB Cells	∿2	2 mil 7070 glass	None	None

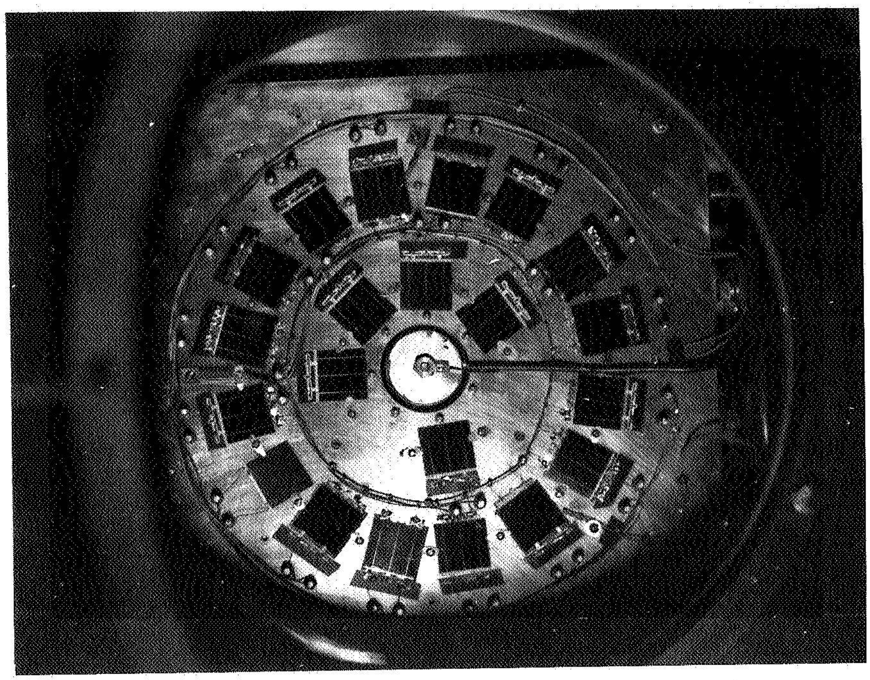

Figure 1. Test Cells Mounted in Test Chamber as Viewed Through Chamber Window.

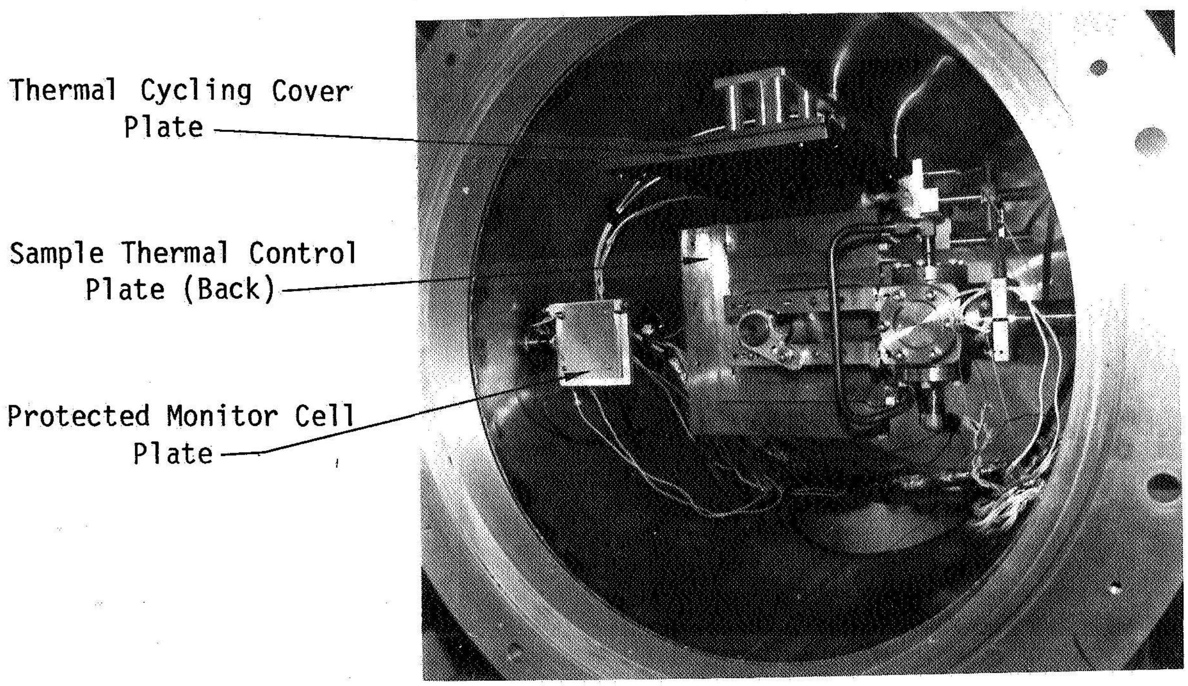

Figure 2. Inside of Test Chamber Viewed From Back of Chamber (Beam coming out of page)

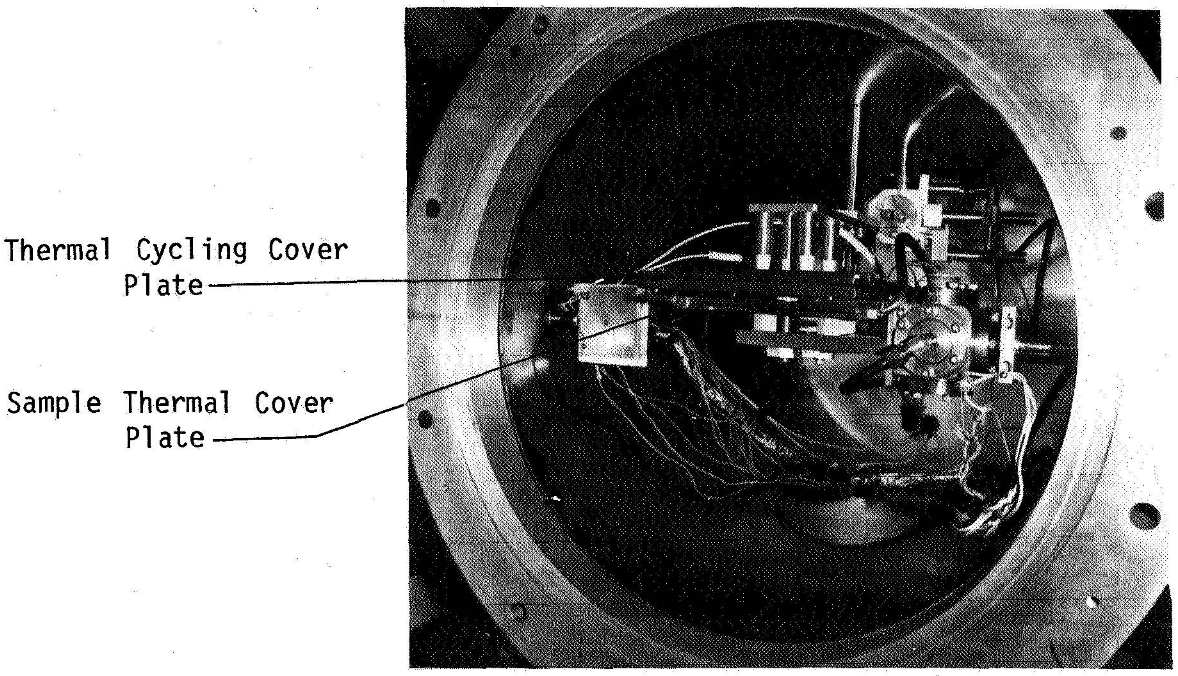

Figure 3. Inside of Test Chamber With Sample Plate in Thermal Cylcing Position.

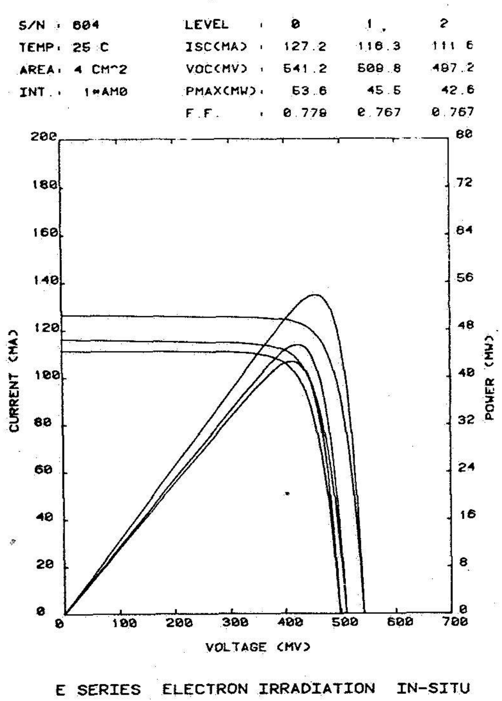

Figure 4. Computer Plotted I-V and Power Curves.

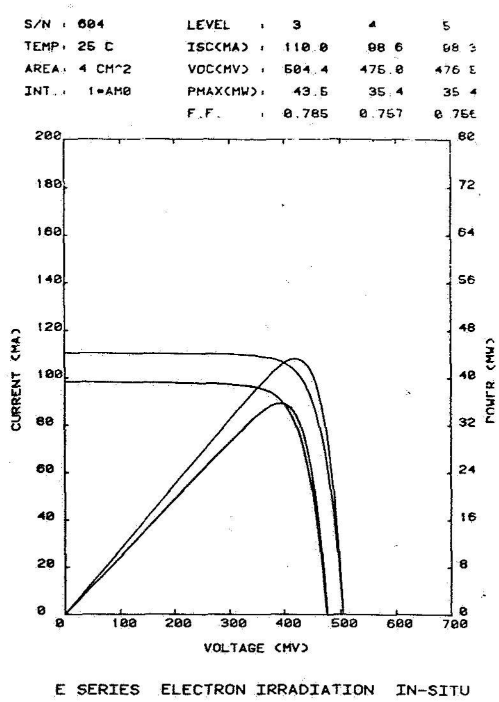

Figure 5. Computer Plotted I-V and Power Curves.

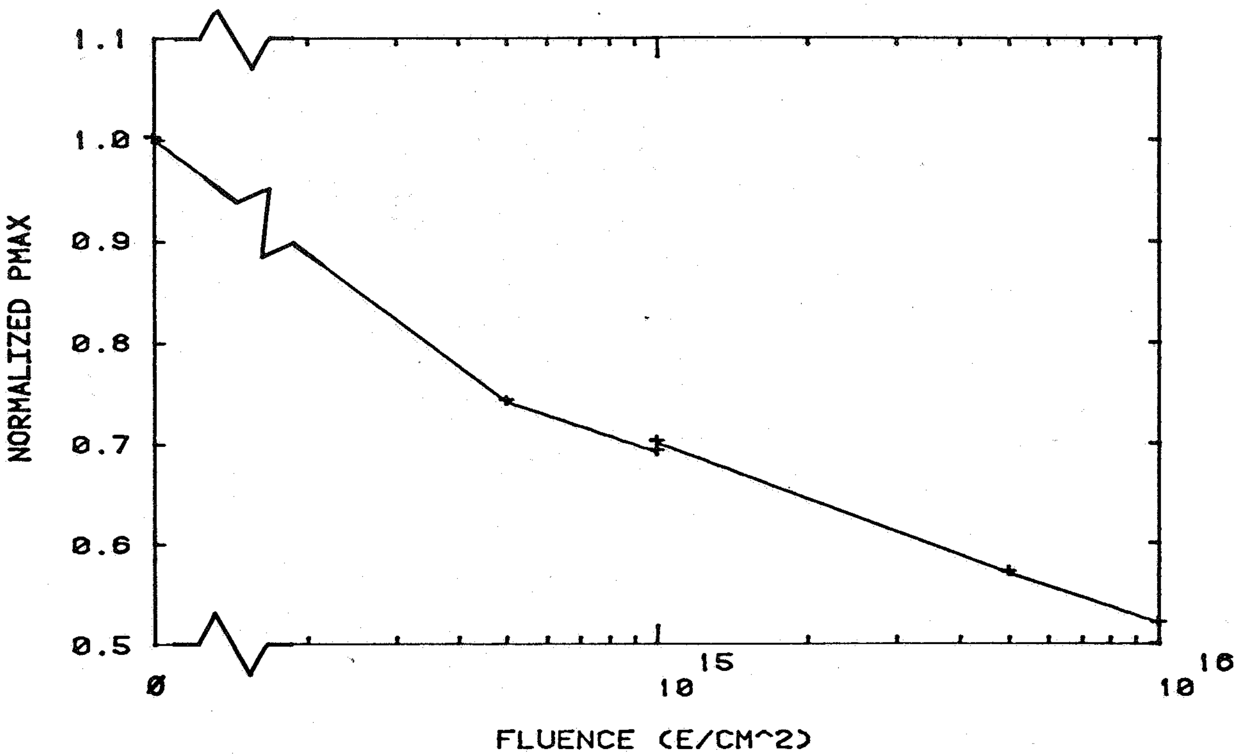

Figure 6. Normalized P_{max} vs. Fluence for A-Series Cells - Electron Test.

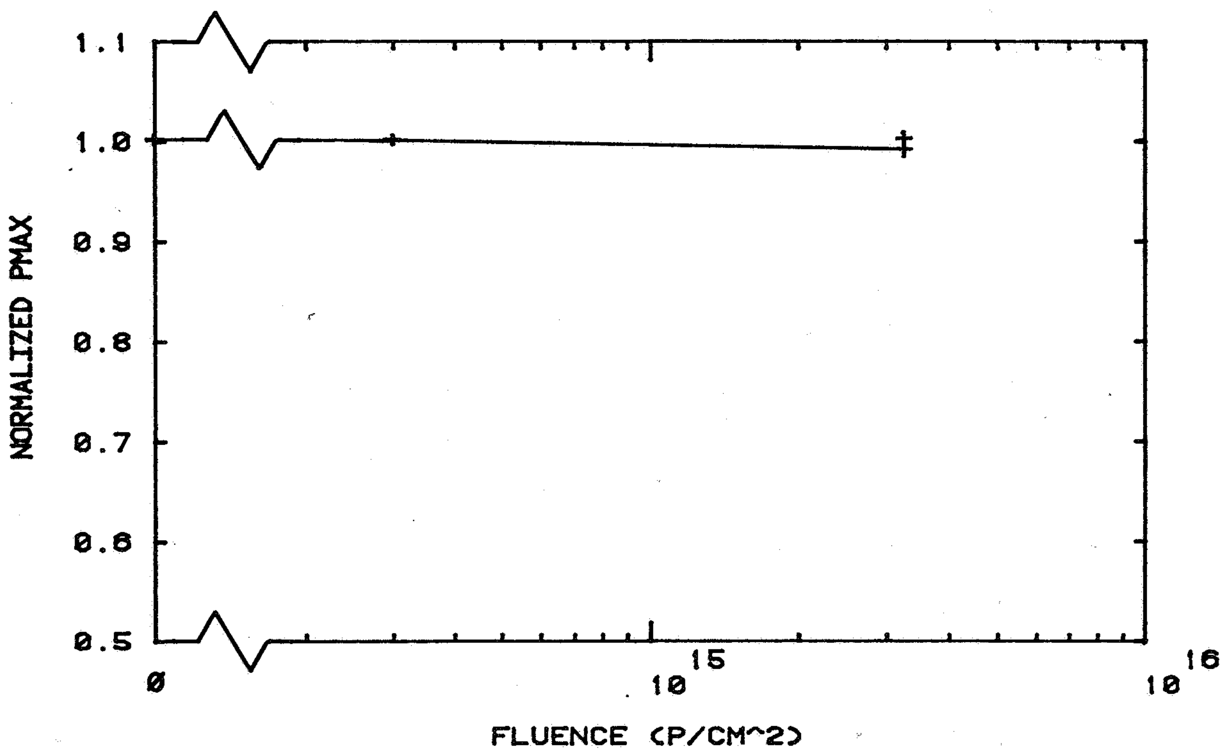

Figure 7. Normalized P_{max} vs. Fluence for A-Series Cells - Proton Test.

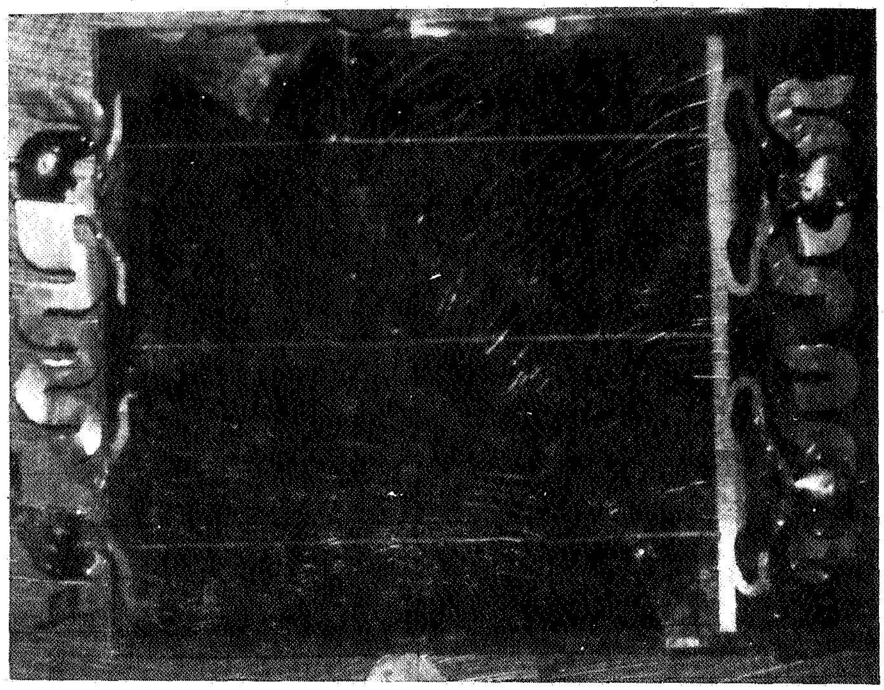

Figure 8. C-Series Cell at Completion of Electron Test.

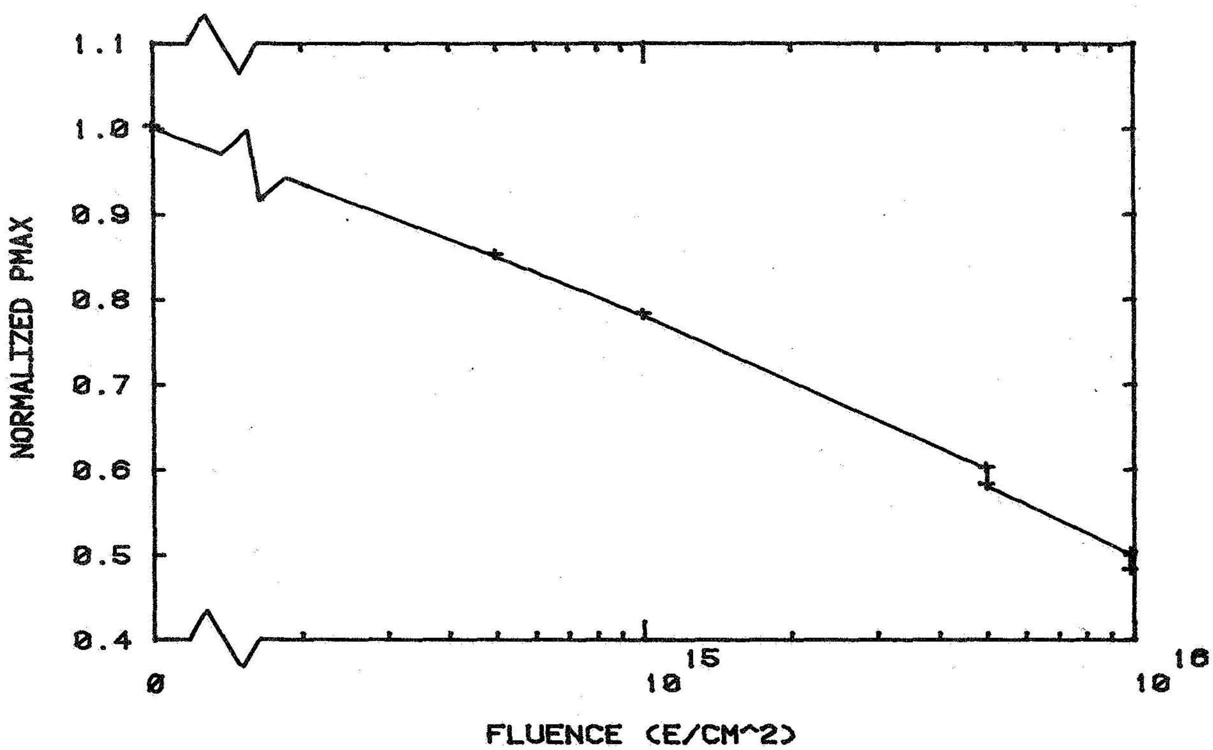

Figure 9. Normalized P_{max} vs. Fluence for C-Series Cells - Electron Test.

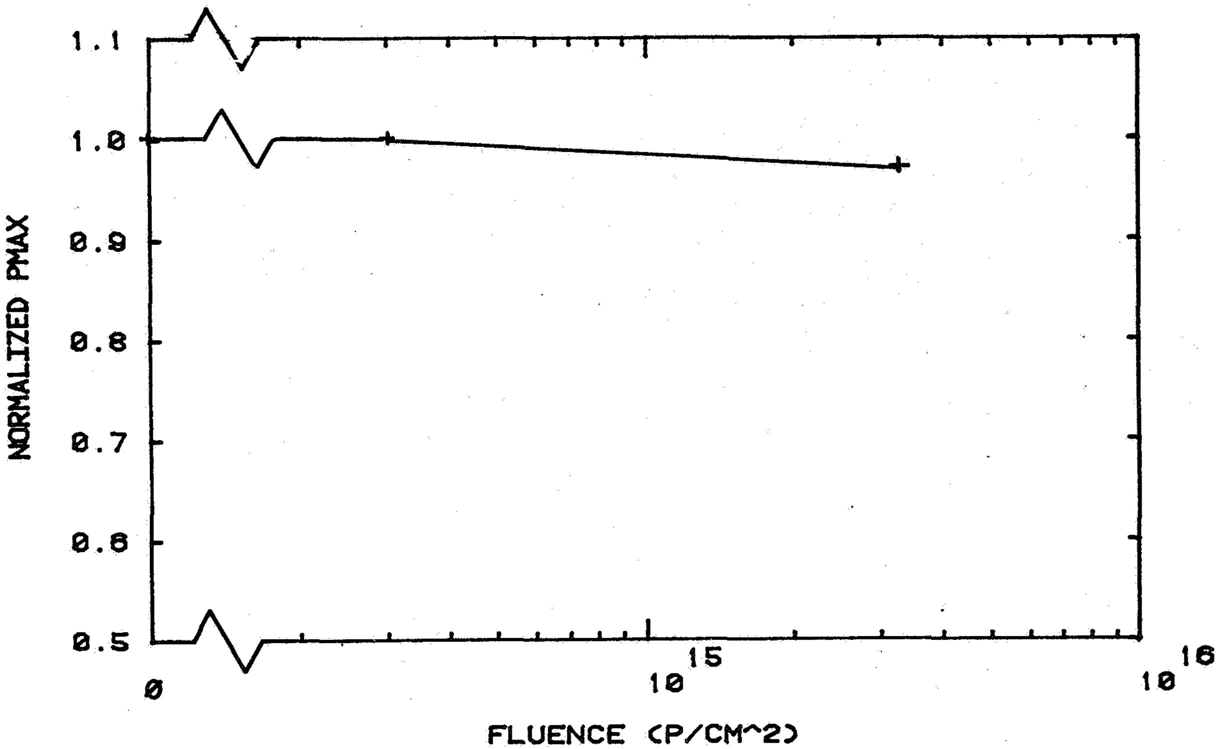

Figure 10. Normalized P_{max} vs. Fluence for C-Series Cells - Proton Test.

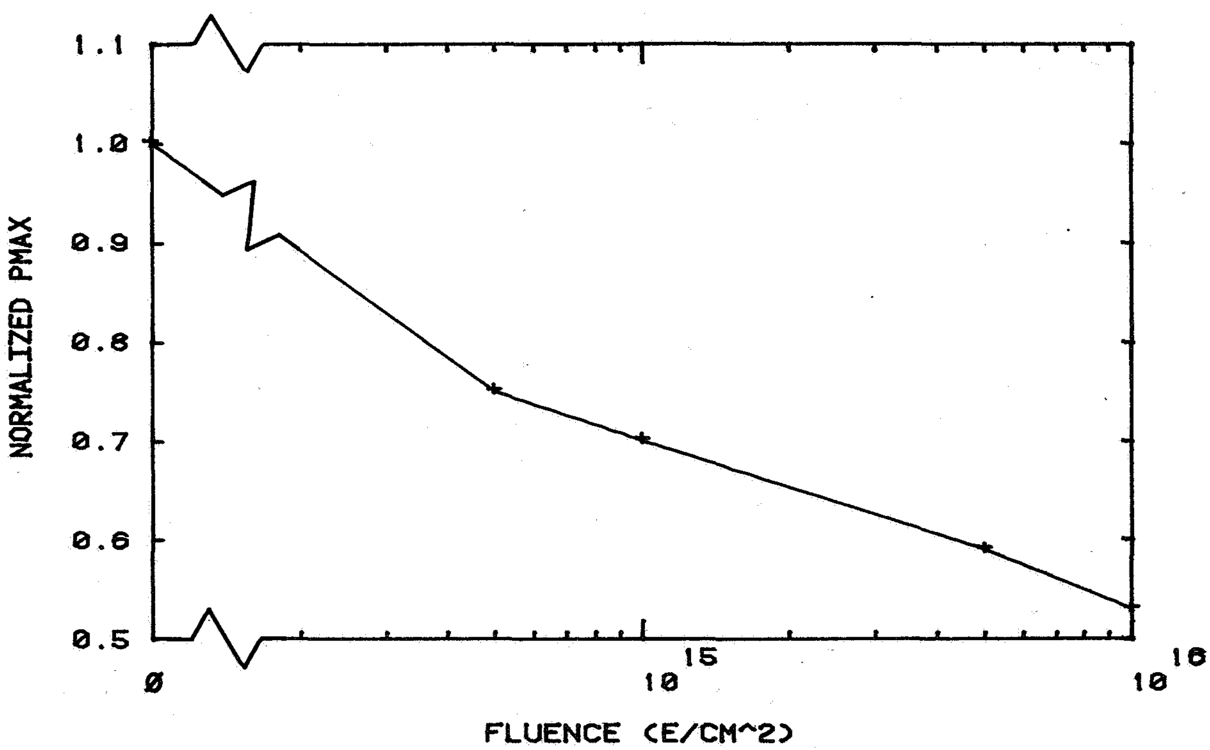

Figure 11. Normalized P_{max} vs. Fluence for D-Series Cells - Electron Test.

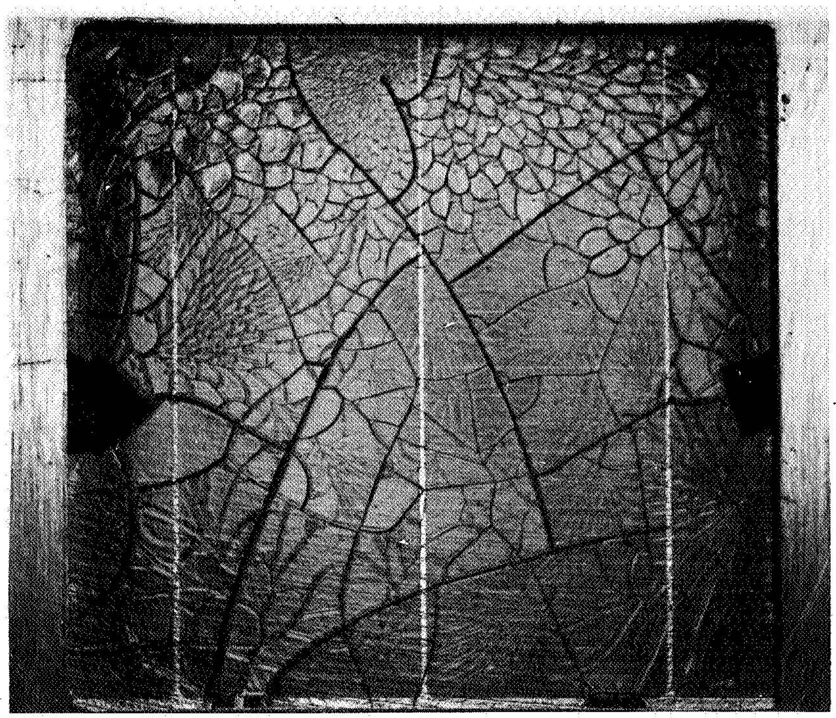

Figure 12. D-Series Cell at Completion of Proton Test.

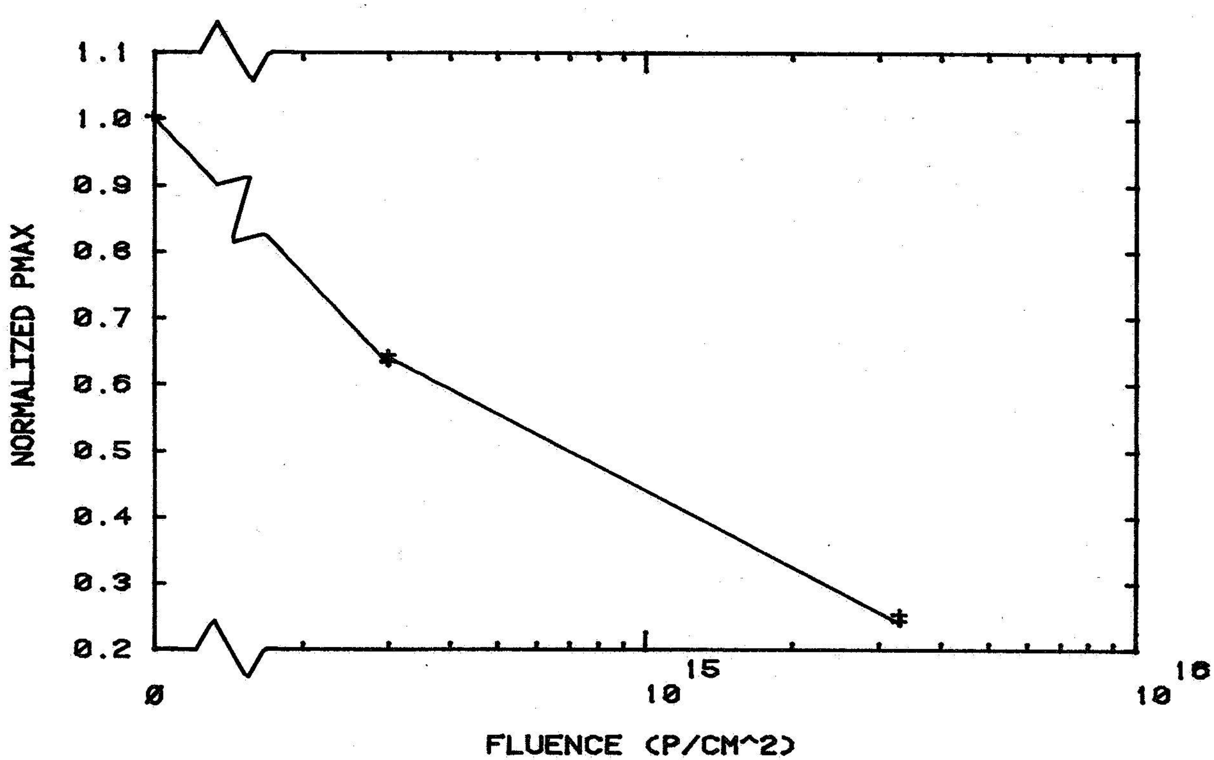

Figure 13. Normalized P_{max} vs. Fluence for D-Series Cells - Proton Test.

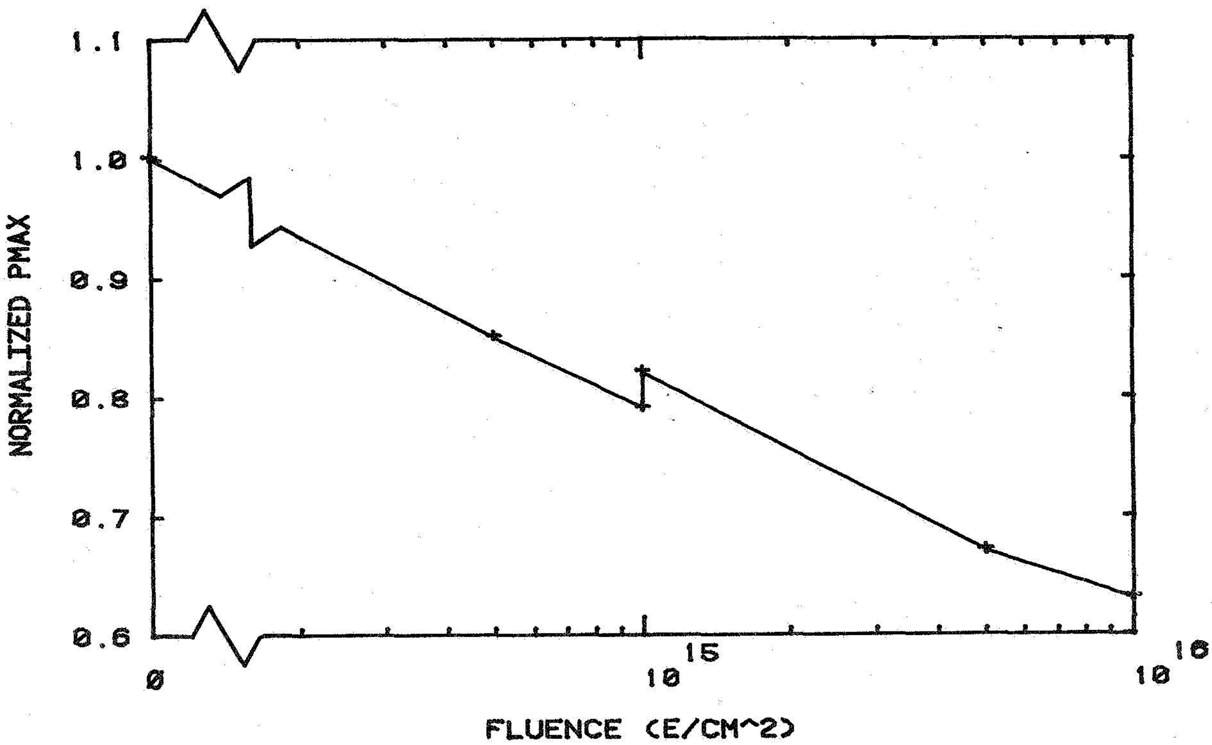

Figure 14. Normalized P_{max} vs. Fluence for E-Series Cells - Electron Test.

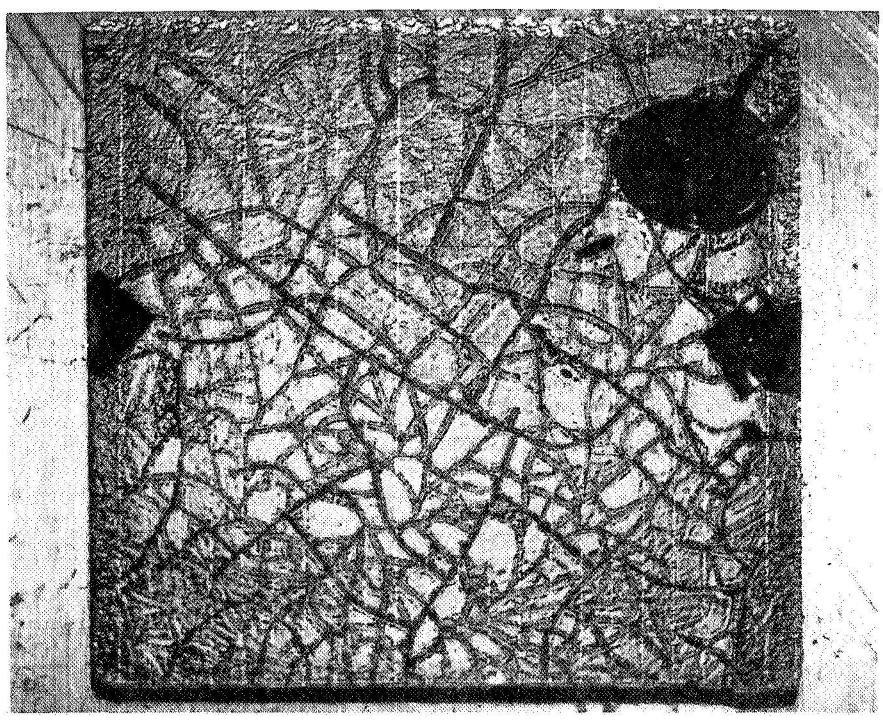

Figure 15. E-Series Cell at Completion of Proton Test.

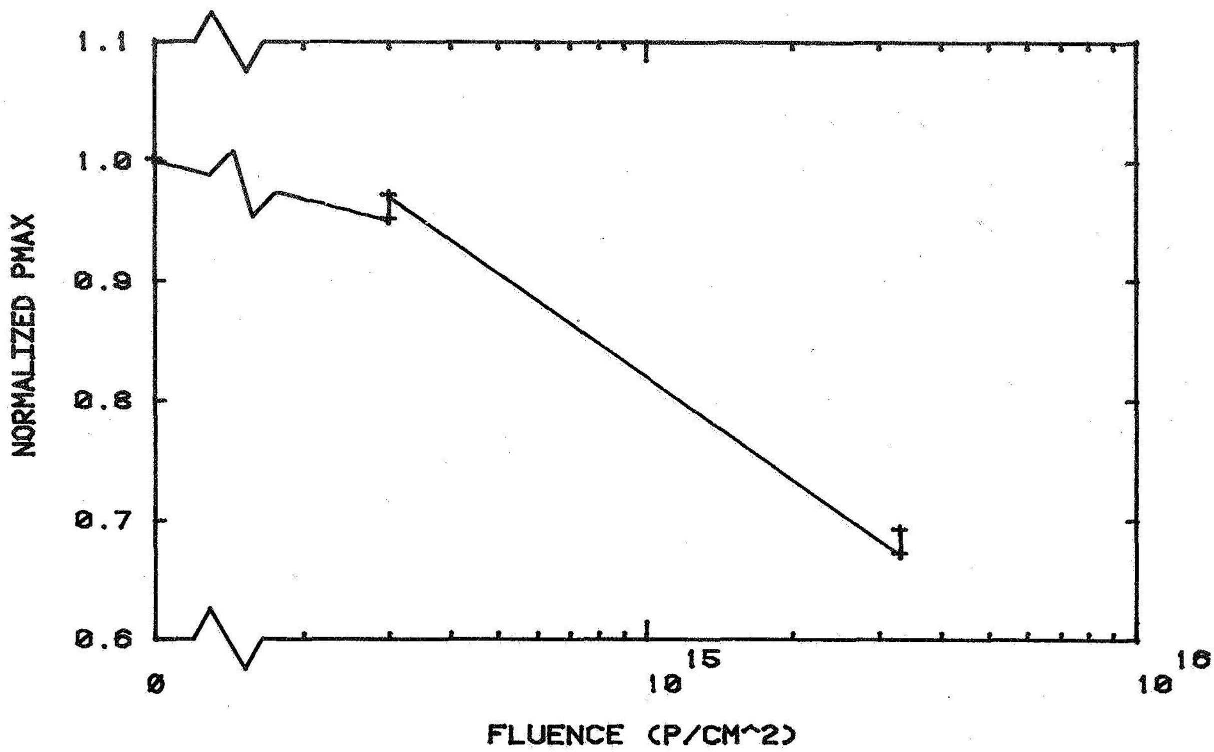

Figure 16. Normalized P_{max} vs. Fluence for E-Series Cells - Proton Test.

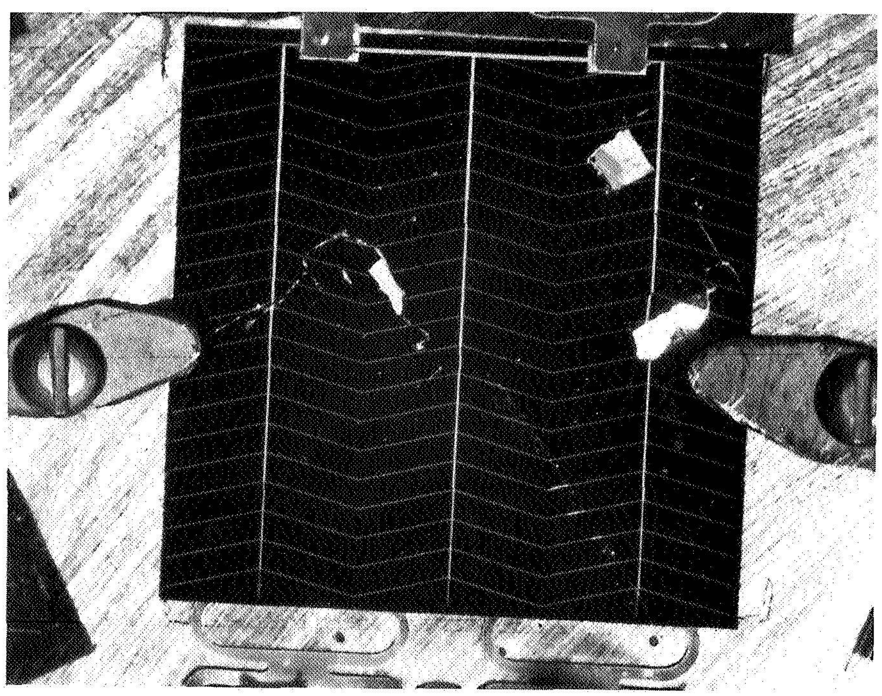

Figure 17. P-Series Cell at Completion of Electron Test.

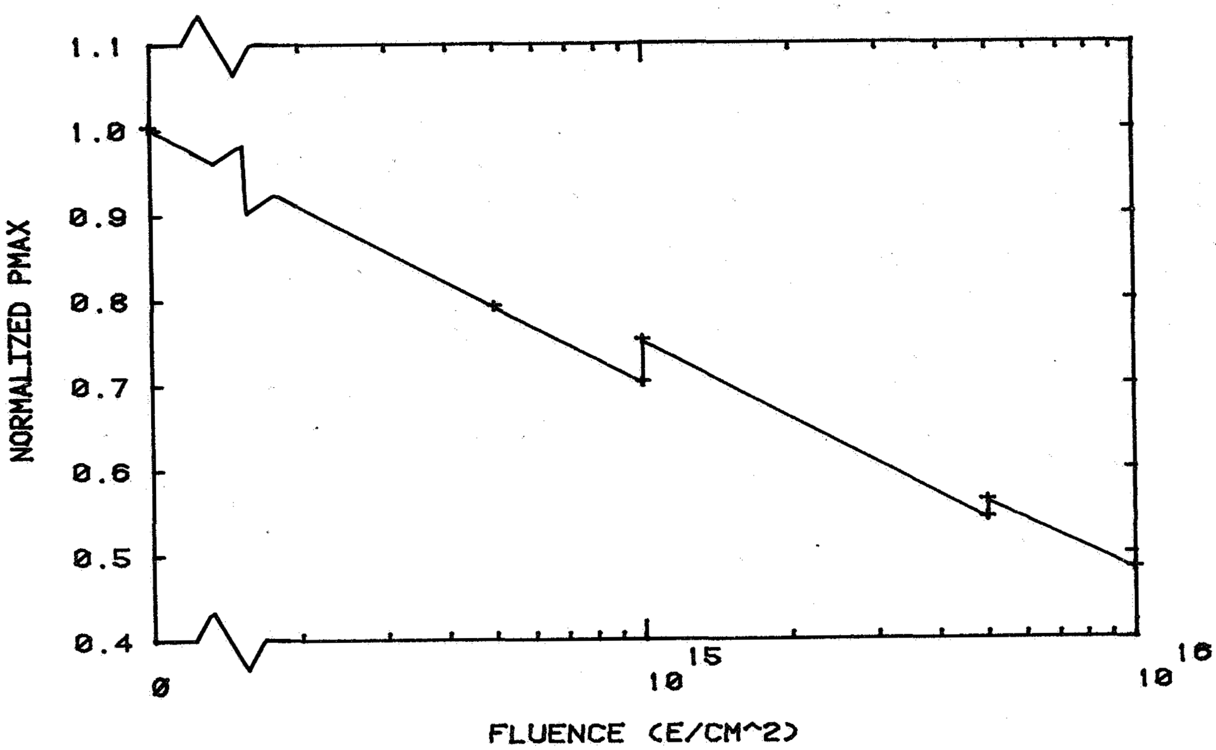

Figure 18. Normalized P_{max} vs. Fluence for P-Series Cells - Electron Test.

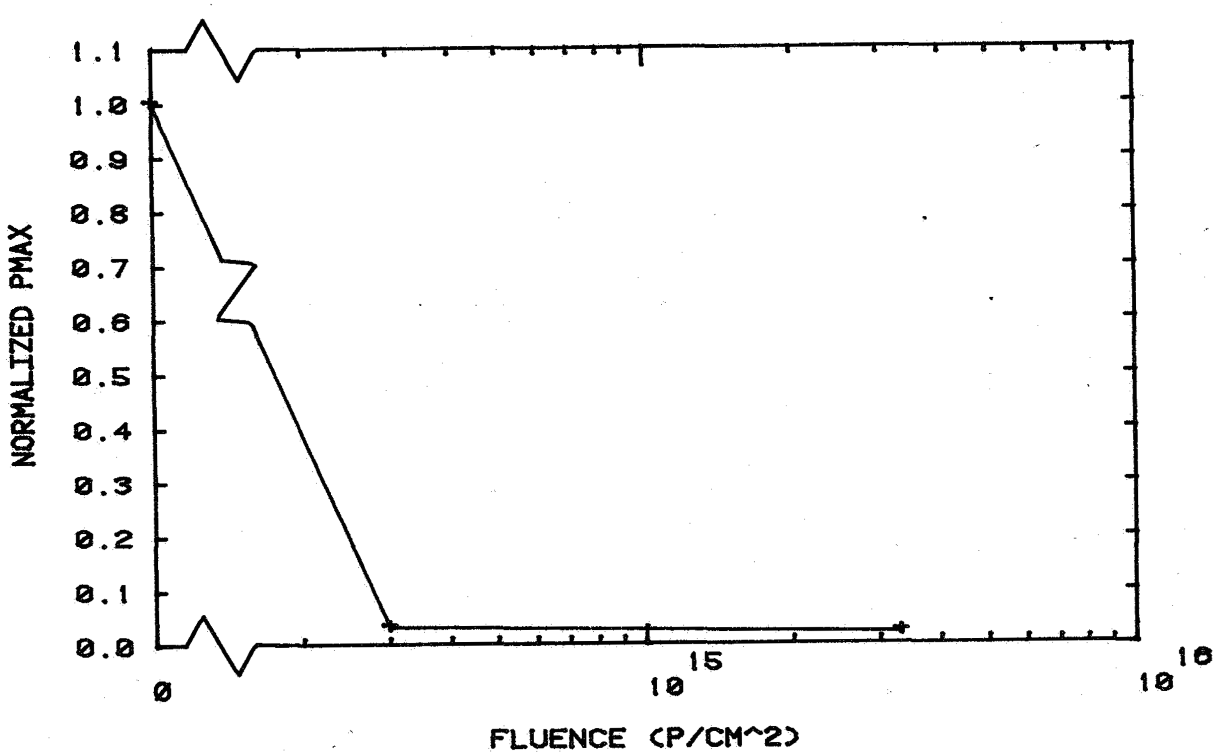

Figure 19. Normalized P_{max} vs. Fluence for P-Series Cells - Proton Test.

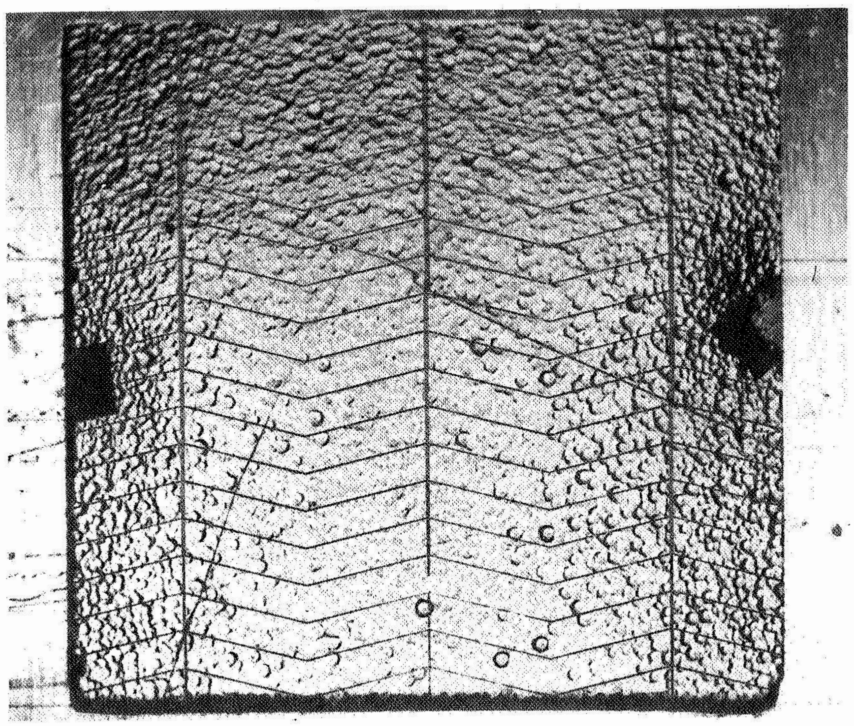

Figure 20. P-Series Cell at Completion of Proton Test.

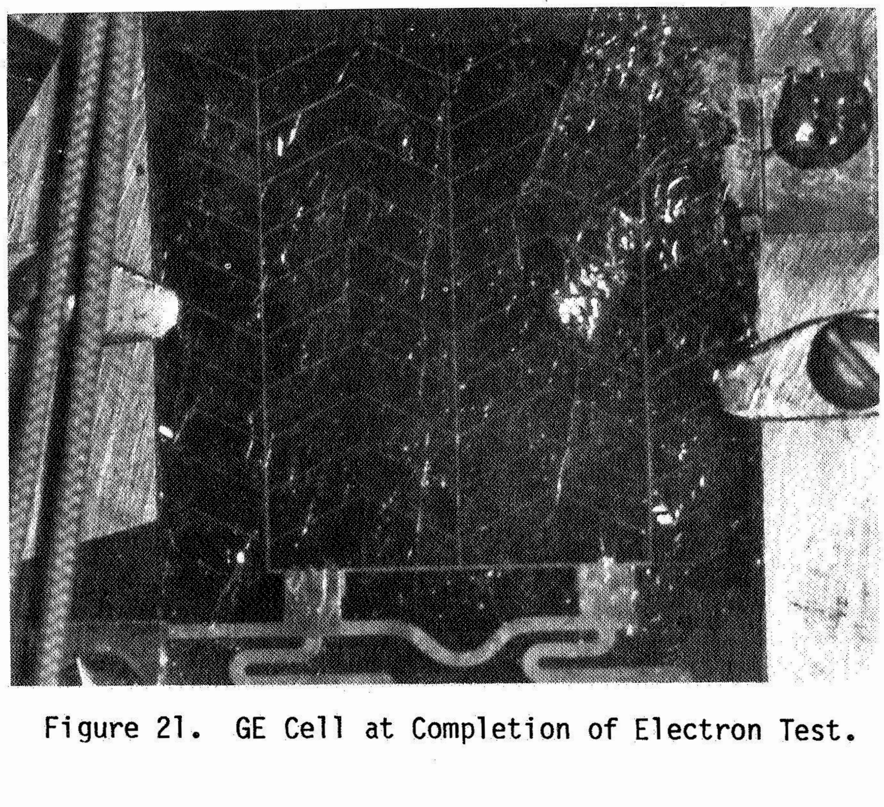

Figure 21. GE Cell at Completion of Electron Test.

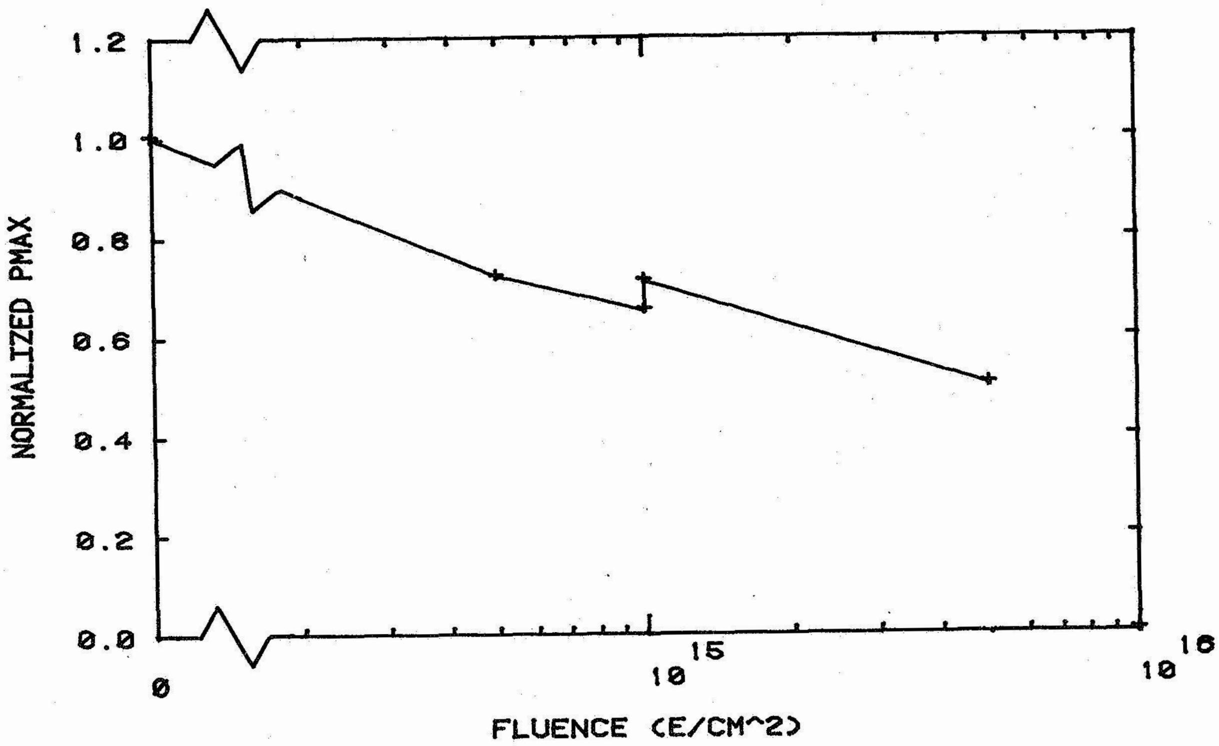

Figure 22. Normalized P_{max} vs. Fluence for GE Cells - Electron Test.

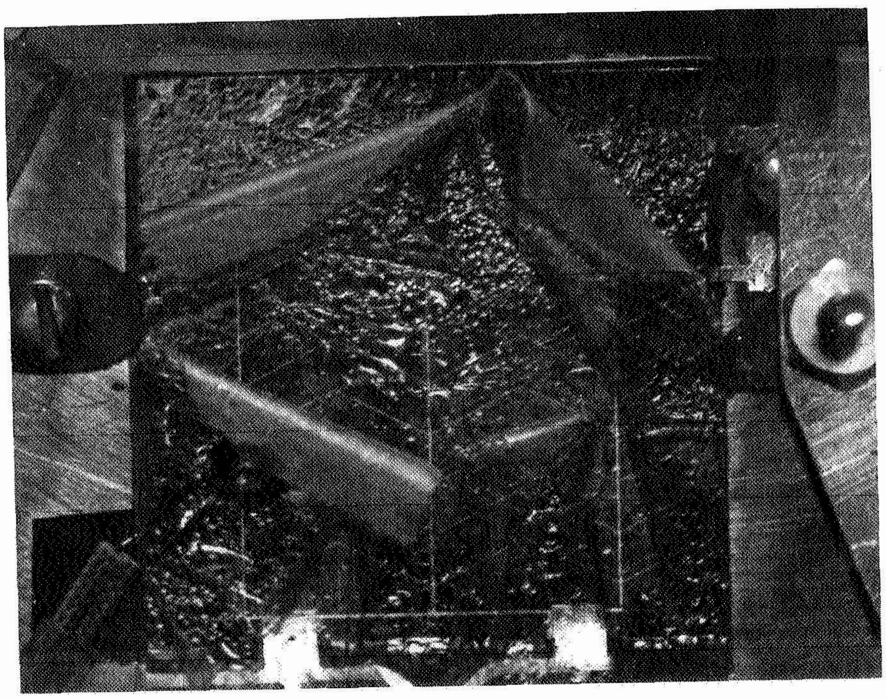

Figure 23. GE Cell at Completion of Proton Test.

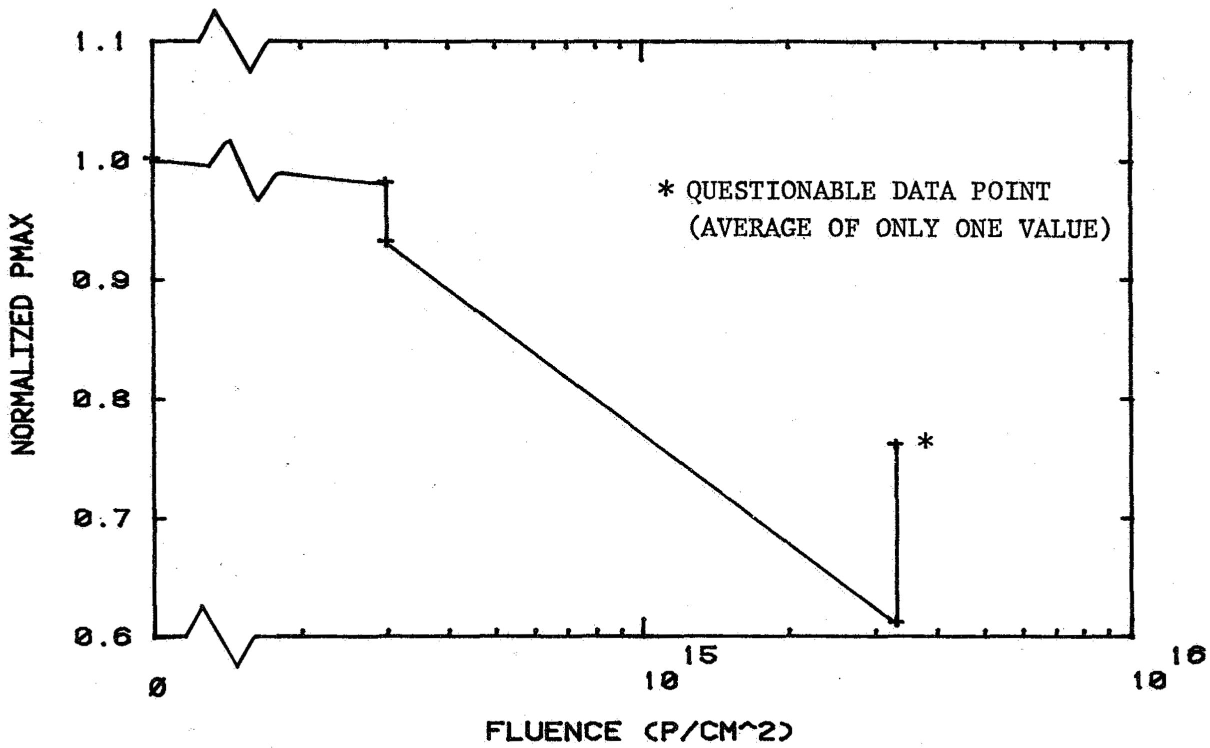

Figure 24. Normalized P_{max} vs. Fluence for GE Cells - Proton Test.

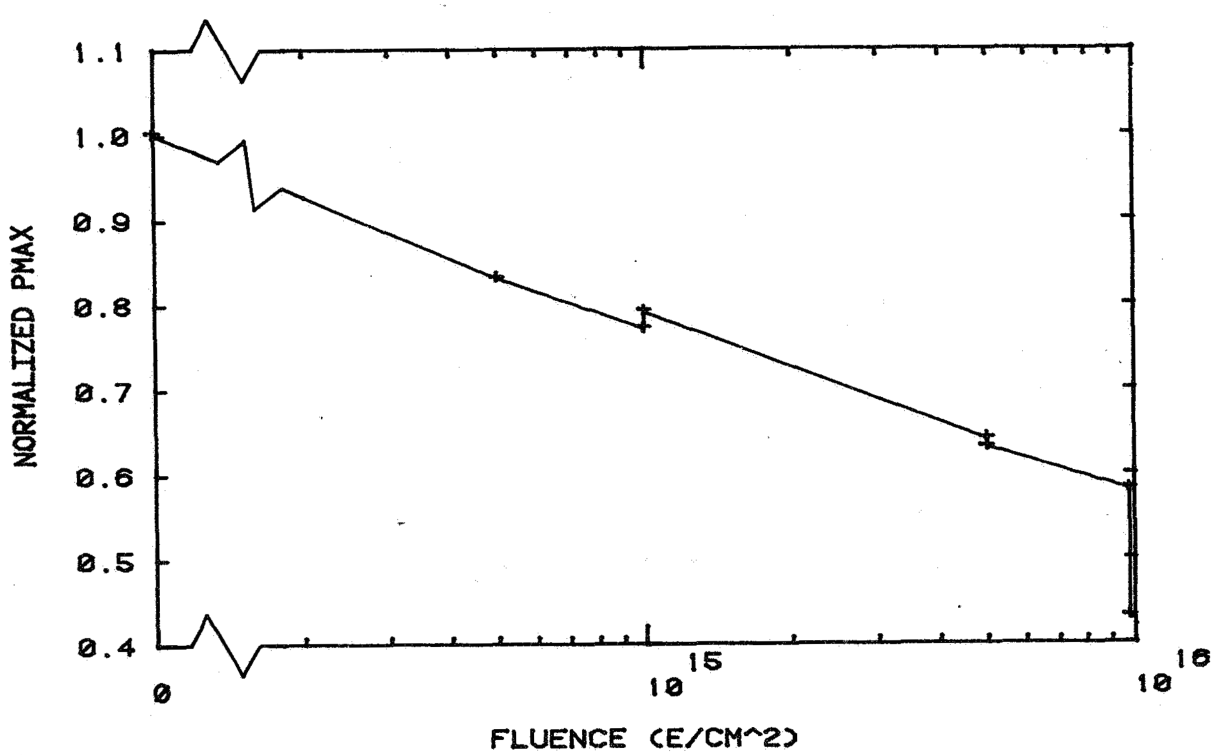

Figure 25. Normalized P_{max} vs. Fluence for Double-Number Cells - Electron Test.

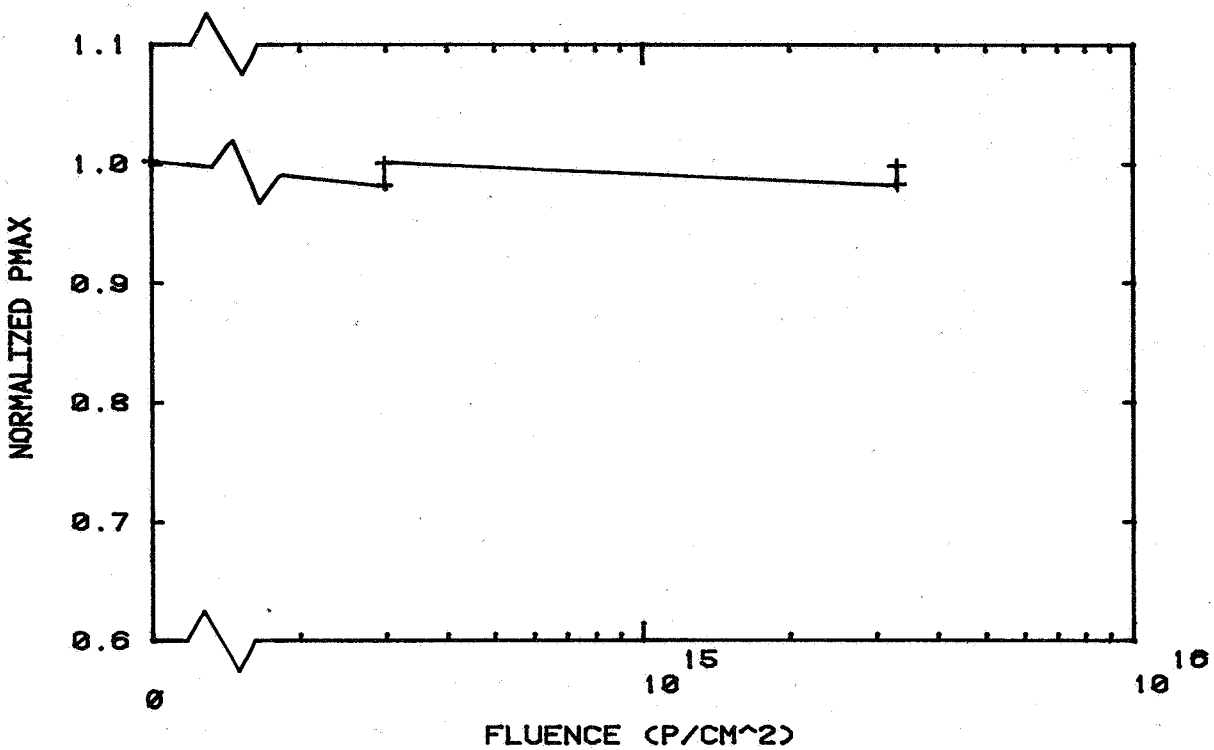

Figure 28. Normalized P_{max} vs. Fluence for ESB Cells - Proton Test.

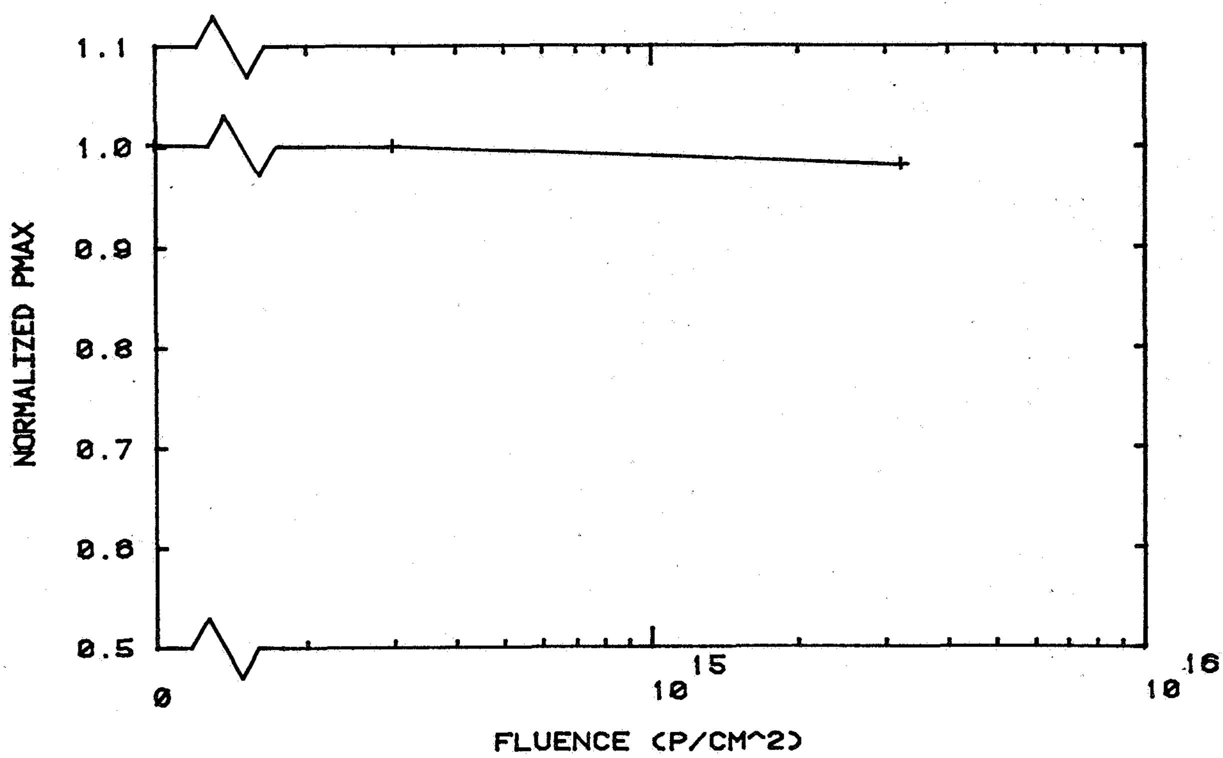

Figure 26. Normalized P_{max} vs. Fluence for Double-Number Cells - Proton Test.

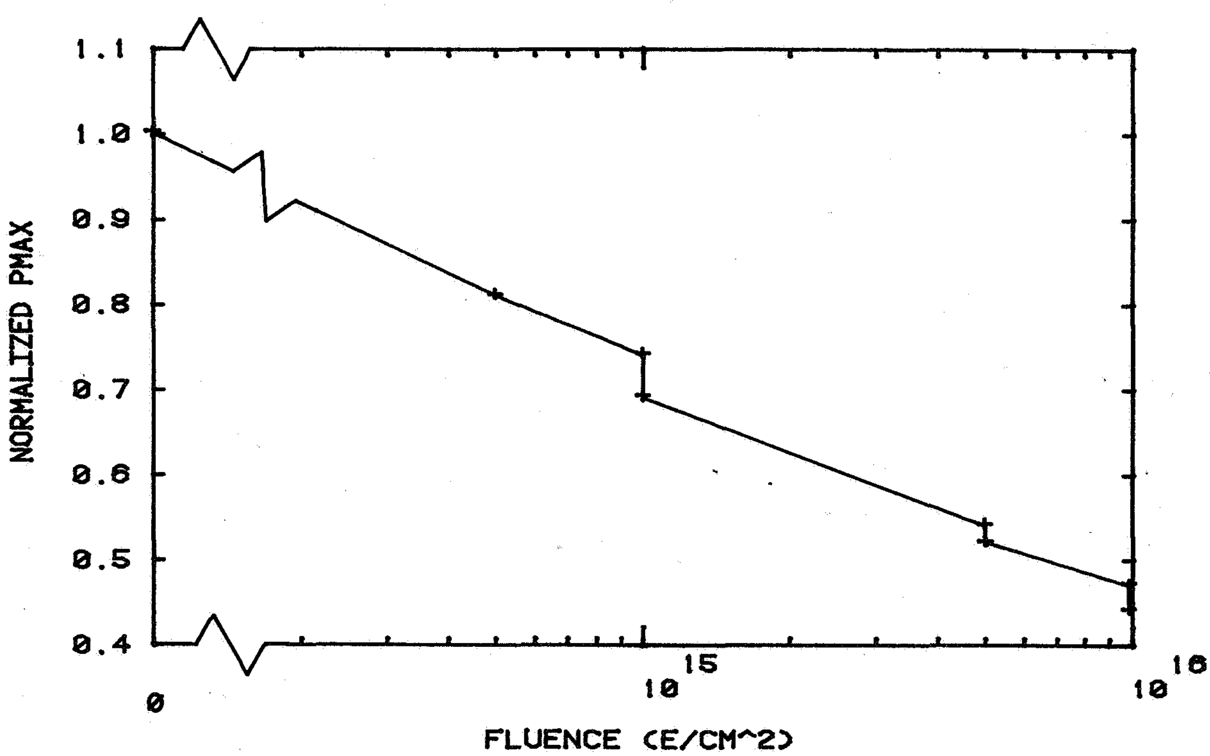

Figure 27. Normalized P_{max} vs. Fluence for ESB Cells - Electron Test.